https://doi.org/10.5194/egusphere-2025-3535
Preprint. Discussion started: 16 September 2025

Climate impact of contrail cirrus from hydrogen combustion aircraft

Susanne M. Pettersson[1], Christian Azar[1], and Daniel J.A. Johansson[1]

[1]Department of Space, Earth and Environment, Chalmers University of Technology, Maskingränd 2, 412 58 Gothenburg, Sweden.

Correspondence: Susanne M. Pettersson (susannep@chalmers.se)

Abstract. To mitigate the climate impact of aviation, combustion of hydrogen as a fuel is one possible future pathway. Hydrogen combustion leads to zero carbon emissions in the exhaust, representing a major step toward climate neutrality, although the non-CO_2 effects, primary contrail cirrus remain uncertain. In this study, we simulate the climate impact, in terms of energy forcing, of contrail cirrus from hydrogen combustion aviation using a modified version of the Contrail Cirrus Prediction model (CoCiP).

Without soot in the exhaust from hydrogen combustion, contrail ice particles instead form on ambient aerosols entrained into the plume and on lubrication oil droplets in the exhaust. The formation of ice particles are modelled using an emulator developed from a theoretically based microphysical contrail formation model.

Following the Schmidt Applemann criterion, hydrogen combustion enables contrail formation at lower altitudes and higher temperatures than fossil jet fuel. However, we find a significant reduction in contrail energy forcing. This result holds across a wide range of assumptions, including different oil particle size distributions and properties, with a global average reduction of about 70% using our base case assumptions. We conclude that hydrogen aircraft not only eliminates CO_2 emissions but may also substantially reduce the climate impact of contrail cirrus, although the reduction and magnitude depend on engine design for lubrication oil handling.

1 Introduction

Contrails are artificial ice clouds that can form behind aircraft (Schumann, 1996). They are initially line-shaped but can under certain conditions, if the ambient air is humid enough, persist and evolve into more naturally shaped clouds. Such evolved contrails are referred to as contrail cirrus. As clouds contrail cirrus affect earth's radiative balance by reflecting incoming sunlight and trapping outgoing infrared radiation (Yang et al., 2010). Depending on a range of factors, such as the time of day, the prevalence of natural clouds and surface albedo, contrail cirrus can either act net cooling or net warming. Estimates of the effective radiative forcing of global aviation show that the warming effect dominates. Although contrail cirrus are short-lived, on the order of hours, maybe a day, their current contribution to aviation effective radiative forcing (ERF) is estimated to two thirds of the total aviation ERF, albeit with a large uncertainty (Lee et al., 2021). Because of aviations valuable contribution of connecting the globe but significant contribution to climate change with approximately 3.5% of global anthropogenic climate

https://doi.org/10.5194/egusphere-2025-3535
Preprint. Discussion started: 16 September 2025

forcing (Lee et al., 2021), possible routes for contrail mitigation are important to map out. Rerouting aircraft around contrail forming regions (Kölker et al., 2024; Rosenow and Fricke, 2018) and strategic usage of low aromatic fuels (Teoh et al., 2022b; Quante et al., 2024) have been suggested as possible options.

The magnitude of contrail cirrus radiative forcing (RF), in addition to the above mentioned circumstances, depend on the properties of the contrail cirrus. A higher density of ice particles (all else equal) increases the contrail lifetime and optical depth (Lewellen et al., 2014; Kärcher, 2016). The density of ice particles in turn depends on particle number and their properties at the contrail's formation (Kärcher, 2016; Yu et al., 2024). Reducing particle number is suggested as a contrail cirrus mitigation strategy in itself, but also comes as a co-benefit of a transition to hydrogen fuel aircraft. Hence, hydrogen combustion, besides no exhaust CO_2 emissions, might be beneficial because of its decreased number of particles in the exhaust. A hypothesis is that the lack of soot and other fossil jet fuel related particles in the exhaust of hydrogen aircraft will reduce the ability of ice particle formation leading to less contrails and a reduced need for rerouting with extra fuel costs.

However, there is uncertainty whether the lack of soot in hydrogen aircraft exhaust will lead to a reduction of ice particles or not. Although lacking in soot and other volatile particle matter/substances such as chemi-ions and sulfates, the hydrogen exhaust contains additional water vapour that will increase the conditions over which contrails can form. The extra water vapour might also increase the amount of ice particles that can form from the particles still present and thereby increase both the occurrence and energy forcing of contrail cirrus (Schumann, 1996). No results from measurement campaigns on contrail cirrus of hydrogen fuelled aircraft have been published yet. However, several measurement campaigns testing blends of conventional jet and Sustainable Aviation Fuels (SAFs) to different degree find a reduced number of ice particles (Voigt et al., 2021) because of the reduction in soot particles (due to reduced aromatics in the fuel) (Moore et al., 2017; Durdina et al., 2021; Zhang et al., 2022). But with even lower soot emissions than in these campaigns (in the order $< 10^{13}$) there are indications of an increase in ice particles at low temperatures due to the activation of other ultrafine particles in the exhaust (Kärcher and Yu, 2009; Yu et al., 2024) such as volatile particles (approximately radii < 5 nm) composed of condensable sulfur and organics mainly forming on chemi-ions (Yu and Turco, 1997; Yu et al., 1999; Kärcher et al., 2000) but including homogeneous lubrication oil droplets relevant for hydrogen combustion. Models are now being developed to capture this increase in ice particle formation due to ultrafine particles but the uncertainty is still large.

In a simulation study of contrail formation with hydrogen fuel the loss of soot is shown to, under most circumstances, significantly reduce the amount of ice-particles formed in a three seconds old plume in comparison to fossil jet fuel (Bier et al., 2024). The circumstances under which this does not hold is when temperatures are high, near the critical threshold of contrail formation for jet, or even higher where only contrails from hydrogen are possible. This simulation lets the ice particles form solely on ambient aerosols. It has been recognised, however, that lubrication oil still present in the exhaust of hydrogen aircraft might contribute to ice particle formation in the absence of soot (Bier et al., 2024; Yu et al., 2024). Soot does not readily act as condensation nuclei for water droplets, lubrication oil droplets even less so, although they can under the right conditions (Ponsonby et al., 2024; Lambe et al., 2011). The additional water vapour in the hydrogen exhaust might be enough to activate lubrication oil to form water droplets.

https://doi.org/10.5194/egusphere-2025-3535
Preprint. Discussion started: 16 September 2025

This study provides the first investigation of the combined effects of additional water vapour from hydrogen combustion and the potential of lubrication oil and ambient aerosols to serve as ice nuclei in contrail formation and their radiative impact from hydrogen-powered aircraft.

The role of lubrication oil and ambient aerosols as ice nuclei is unfortunately associated with large uncertainties. For the characterisation of lubrication oil in aircraft exhausts all studies published have been conducted on conventional aircraft i.e. kerosene driven craft. Large uncertainties stem from the fact that lubrication oil can be both vented outside the main exhaust stream or be emitted or leaked out in the exhaust at high temperatures. This leads to large differences in oil size distributions, since oil is a volatile substance. In addition to uncertainties in size-distribution lubrication oils' readiness to act as condensation nuclei is uncertain (Lambe et al., 2011). Further uncertainties can be found regarding the amount of lubrication oil emitted depending on oil and engine types (Yu et al., 2010; Timko et al., 2014; Decker et al., 2024).

The designator ambient aerosols covers all types of particles suspended in the atmosphere. Therefore there is a large span of particle types, sizes and properties included in this category leading to large variability and uncertainties in ambient aerosol characterisation (Raes et al., 2000; Clarke and Kapustin, 2002; Minikin et al., 2003) (, hermann, brock, voigt - kolla upp). Ambient aerosols vary in their spatial distributions, size distributions and chemical properties, a trait found in both observation campaigns (Clarke and Kapustin, 2002; Minikin et al., 2003) and emphasized in modelling of aerosol physics in climate models(Stier et al., 2005; Kaiser et al., 2019).

Despite the large uncertainties and variability in both ambient aerosols' number concentration and composition and in the specifications of lubrication oil, we aim in this study to map the contrail cirrus climate impact for a large set of plausible assumptions. In this way we can narrow down the space of possible contrail contribution from hydrogen aircraft. In addition we can contribute with insights to guide the future development of hydrogen engines to avoid designs that can lead to a large contrail impact.

To investigate contrail formation, evolution and energy forcing from hydrogen aircraft we use the Contrail Cirrus Prediction model (CoCiP) (Schumann, 2012). CoCiP in its original formulation forms ice particles solely on soot emissions (or defaults to 10^{13} as a way of accounting for background ambient aerosols if the soot emissions given are lower). We modify the functions of the model covering ice particle activation to include ice particles formed on lubrication oil and ambient aerosols. Given atmospheric conditions, oil emission index and oil properties the newly developed functions estimate the amount of formed ice particles to initiate the contrail cirrus simulation in CoCiP for estimating radiative implications. The amount of oil and ambient aerosols activated to ice particles is based on the theoretical model put forward by Kärcher et. al (Kärcher et al., 2015). This model was originally formulated for soot and ambient aerosols but offers an approach of extending to other types of particles provided their characteristics are given.

2 Theory

A thermodynamic criterion for contrail formation, termed the Schmidt-Appleman Criterion (SAC) after its founders, dates back to the 1940s (Schumann, 1996). It depends on both ambient conditions and fuel exhaust properties. Intuitively, the criterion

https://doi.org/10.5194/egusphere-2025-3535
Preprint. Discussion started: 16 September 2025

requires that the hot exhaust gas from the aircraft engines at some point during its cooling and mixing with ambient air becomes supersaturated with respect to water. The supersaturation enables the formation of water droplets which will subsequently freeze to form the contrail. The so-called mixing line of the exhaust plume, tracing its temperature (T) and partial water vapour pressure (p_w) over time, can be approximated as linear in T-p_w space (excluding a brief non-linear phase right after exit) (Schumann, 1996). The slope of this mixing line is given by

$$G = \frac{c_p EI_{H_2O} p_a}{0.662 Q(1-\eta)}, \tag{1}$$

where c_p is the isobaric specific heat of air, EI_{H_2O} is the mass emission index of water vapour, p_a the air pressure, η the overall propulsion efficiency, Q the specific heat of the fuel and 0.622 is the ratio between the molar masses of water and air. The SAC is then the temperature at which the mixing line is tangential to the saturation curve with respect to water (saturation water vapour pressure curve). Any lower temperature will lead to the mixing line crossing the saturation curve and a period of supersaturation in the plume, while for higher temperatures no supersaturation with respect to water will be reached. In general, the steeper the slope of the mixing line G the higher the supersaturation in the plume for the same ambient conditions and the more water available to form droplets. The mass emission index of water vapour and the specific heat of the fuel have a large influence on G as can be seen from Eq. (1). For jet-A fuel we have $\mathrm{EI_{H_2O,J}} = 1.23$ kg (kg fuel)$^{-1}$ and $\mathrm{Q_J} = 43.2$ MJ (kg fuel)$^{-1}$ in comparison to $\mathrm{EI_{H_2O,H_2}} = 8.96$ kg (kg fuel)$^{-1}$ and $\mathrm{Q_{H_2}} = 123$ MJ (kg fuel)$^{-1}$ for hydrogen. All else equal this gives a slope for hydrogen approximately 2.6 times steeper than for standard Jet-A fuel. In addition, to larger supersaturations in the plume at the same ambient temperatures, the steeper slope for hydrogen as fuel also enables contrail formation at higher ambient temperatures approximately 10K above conventional Jet-A fuel (Schumann, 1996).

The Schmidt-Applemann criterion predicts quite accurately when contrails form, but for the contrail to persist, the ambient air needs to be supersaturated with respect to ice. If both these criteria are fulfilled, a contrail can form, persist, and potentially evolve into a contrail cirrus. Also, the properties of the persistent contrail/contrail cirrus depend on the amount and type of particles present for activation into water droplets. With a larger number of particles present, a larger number of droplets can form. The amount of water droplets will also depend on the readiness of the present particles to act as condensation nuclei, that is, their hygroscopicity and size distribution. The hygroscopicity of substances can be roughly captured with a single parameter κ (Petters and Kreidenweis, 2007) and for ambient particles it lies in the range $\kappa = 0.1$-0.9 (Petters and Kreidenweis, 2007). The higher the κ of a substance, the lower the supersaturation required for it to act as condensation nuclei for water droplets. Same for size, the smaller the initial aerosol the higher the supersaturation required for it to act as condensation nuclei for water droplets. The κ-Köhler equation gives the water saturation ratio S (where supersaturation s is saturation ratio minus one $s = S - 1$) for the equilibrium wet diameter D for a particle/solution of dry diameter D_d

$$S(D) = \frac{D^3 - D_d^3}{D^3 - D_d^3(1-\kappa)} \cdot e^{\left(\frac{4\sigma_{s/a} M_w}{RT\rho_w D}\right)}, \tag{2}$$

where $\sigma_{s/a}$ is the surface tension of solution/air interface, ρ_w the density of water, M_w the molecular weight of water, R the universal gas constant and T the temperature. The exponential part of eq. 2 instantiates the Kelvin effect which describes how

https://doi.org/10.5194/egusphere-2025-3535
Preprint. Discussion started: 16 September 2025

the saturation water vapour pressure increases over a curved surface. As can be seen the exponential approaches infinity as the wet diameter approaches zero (curvature increases), this is because less energy is needed for a water molecule to evaporate the more curved a surface is and therefore the equilibrium saturation water vapour pressure is increased. The maximum of the κ-Köhler curve gives the critical saturation ratio S_c, the minimum saturation ratio needed for a particle with a certain dry diameter and κ to grow indefinitely according to theory (although being limited by the atmospheric water budget in reality) or equivalently the minimum dry diameter needed at a certain saturation ratio. The minimum dry diameter/radius is referred to as the activation diameter/radius r_{act} and particles with $r > r_{\text{act}}$ in an environment with $S > S_c$ are said to be activated. Because of the Kelvin effect the critical saturation ratio for small particles is increased, a small κ is also seen from Eq. (2) to increase the critical saturation ratio for a certain dry radius.

3 Models and implementation

For our investigation into contrail formation and the climate impact of hydrogen aircraft, we use two models. To approximate the amount of ice particles formed in the exhaust under various conditions we use the theoretical model put forward by Kärcher et. al (Kärcher et al., 2015) (subsequently referred to as K15) but modify it to account for particles with a very low hygroscopicity using the κ-Köhler model (Petters and Kreidenweis, 2007). The number of ice particles predicted in this way is then used as input for CoCiP (Contrail Cirrus Prediction model) constructed by Schumann (Schumann, 2012) for simulating contrail lifetime and its radiative impacts.

3.1 Theoretical model for ice particle formation, κ-köhler theory and activation emulators

3.1.1 Particle activation - model overview

The K15 model has the capacity to predict microphysical and optical properties of contrail particles the first few seconds after exhaust. The model predicts, among other things, the number of ice particles that form from exhaust and entrained particles given ambient conditions, engine parameters and the particles' properties, emission numbers or ambient concentrations. The relations between particle size, hygroscopicity, saturation ratio and activation is given by an approximation to κ-Köhler theory in Eq. (2), and the saturation ratio in the plume over time is given by the ratio of the partial water pressure for the mixing line over the saturation water vapour pressure curve. The K15 model approximates the number of water droplets formed by equating on the one hand the possible number of droplets that can form at a certain supersaturation along the mixing line (Eq. (37) in K15) with on the other hand the number of these particles needed to deplete the supersaturation at the point when the production rate of supersaturation equals the loss of supersaturation due to condensation (Eq. (51) in K15). The time when these two calculations of droplet particle numbers are equal the particles are said to "quench" the supersaturation of the plume and no more particles can be activated into water droplets. The plume might still be supersaturated with respect to water after quench although not enough to activate the remaining unactivated particles. With the remaining supersaturation the formed droplets can continue to grow by condensation until the supersaturation is completely depleted or the plume reaches

https://doi.org/10.5194/egusphere-2025-3535
Preprint. Discussion started: 16 September 2025

the freezing temperature estimated by K15 (Eq. (36) in (Kärcher et al., 2015)), at which point droplets freeze into ice particles. Thus the number of water droplets at quench equals the number of ice particles formed.

A crucial difference between the model and actual formation of water droplets from plume aerosols is that in reality droplets would form continuously and successively deplete the supersaturation leading to a decreasing ability to activate particles with low hygroscopicity and/or small radius. The model may therefore overestimate the activation of small or low-hygroscopicity exhaust particles because of lower ability to activate and due to an underestimation of the competition for water between ambient aerosols and exhaust particles, since lower supersaturation would promote the activation of ambient aerosols with higher hygroscopicity over small and low-hygroscopicity exhaust particles (Lewellen, 2020).

3.1.2 Activation of lubrication oil particles - approximations

The hygroscopicity of lubrication oil is uncertain but known to be low. In (Ponsonby et al., 2024) it is shown to be consistent with $\kappa = 0$ for droplets of lognormal distribution and mean radius 100 nm, in another study an upper limit for lubrication oil is estimated to $\kappa = 6 \cdot 10^{-4}$ (Lambe et al., 2011). We have implemented a modification to the approximate expression for the critical supersaturation (maximum of Eq. (2)) and activation radius from (Petters and Kreidenweis, 2007) used in K15, to account for the low hygroscopicity of lubrication oil. The original approximate expression in (Petters and Kreidenweis, 2007) is

$$s \approx \ln(S) = \sqrt{\frac{(r_k/r_{act})^3}{54\kappa}}, \tag{3}$$

where s is the supersaturation, S the water saturation ratio, r_k is the Kelvin radius set to 1 in K15 but equal to $r_k = \frac{4\sigma_{s/a} M_w}{RT\rho_w}$ in Petters, M. & Kreidenweis, S. and in our study. This approximation of the relation between the critical supersaturation and activation radius is good for $\kappa > 0.2$ (Petters and Kreidenweis, 2007) but becomes increasingly worse for substances with smaller κ. Our correction to Eq. (3) is non-physical in the sense that it is not derived from first principles but rather based on a minimization of the error between the approximation of Eq. (3) and the critical saturation ratio maximum from Eq. (2) for small κ-values, more details can be found in Supplementary S2. The corrected equation for the activation radius is

$$r_{act} = \alpha_0 \kappa^{\alpha_1} s^{-2/3} \frac{r_k}{(54\kappa)^{1/3}} \tag{4}$$

where $\alpha_0 = 1.16788$ and $\alpha_1 = 0.186086$. We have calibrated the correction such that $\alpha_0 \kappa^{\alpha_1} \approx 1$ for $\kappa = 0.5$. For $\kappa > 0.5$ no correction is needed since Eq. (3) is valid.

The K15 model can incorporate any number of particle types with lognormal size distributions and varying hygroscopicities from either exhaust or the ambient atmosphere. If multiple particle types are present in the plume the model utilises averages of the particle types activation radii r_{act} (and slope parameters, see supplementary S3) for obtaining the quench time, calculated as droplet number weighted averages of the different activated particle types. Thus the model uses averages to obtain the time of quench but also keeps track of the number of each particle type that is activated into water droplets calculated with an estimated activation fraction for each particle type (ϕ_l in K15 Eq. (37) and (40)) multiplied by the number of particles of each type respectively in the plume. Our model implementation needs the number of activated droplets from each particle type at

https://doi.org/10.5194/egusphere-2025-3535
Preprint. Discussion started: 16 September 2025

the time of quench for implementation in CoCiP. Thus we created emulators (or fitted functions) to the activation fraction at quench to use in CoCiP. This is done for shortening runtimes in our updated version of CoCiP since the K15 model does not supply a closed expression for the number of ice particles formed but estimates it from the equality of the two expressions of activated droplets mentioned above (Eq. (37) and (51) in K15). The solution to the equality can be found by numerical methods. Implementation of this for every waypoint in CoCiP would be too time intensive to cover all cases we wish to investigate.

3.1.3 Variation in size distributions and properties

The uncertainty and variability in the lubrication oil particle size distribution is large because of the differences in oil handling by different engines, either vented or leaked, in or beside the exhaust. For volatile lubrication oil in the exhaust this implies it needs time to form droplets which in turn effects the characteristics of the particle size distribution. Larger oil droplets from oil-venting is mostly captured for re-use which in a study gave the remaining vented droplets a volumetric mean radii of 125-175 nm from an experiment of aircraft engines in idle (Yu et al., 2010). A measuring campaign around Narita airport in Japan reported smaller size distributions of radii < 15 nm (Fushimi et al., 2019). Experiments using lubrication oil heated to two different temperatures and measured at room temperature show mean diameters of approximately $\sim$10 nm and 27 nm for temperatures at 300°C and 20°C respectively (Ungeheuer et al., 2022).

To handle the variability in size distribution our emulator for lubrication oil activation includes mean μ_o and variance σ_o^2 of the lognormal size distributions, as well as variables related to ambient conditions, which include ambient temperature T_a, relative humidity rh, air pressure p_a and critical saturation temperature T_c (from SAC). Hygroscopicity in terms of κ value was not included as a variable in the emulator, to limit the functional complexity, but the functional form of the emulator can be made to fit different κ, more details of method to find functional form, parameters and span of validity can be found in supplementary S3.1.

There is also a large variability in ambient aerosols (Raes et al., 2000; **?**; **?**; **?**; **?**). The largest source of upper tropospheric aerosols come from anthropogenic and natural emissions of precursors carried to high altitudes by updrafts (Minikin et al., 2003) which later form particles, but also from for example aircraft emissions (Righi et al., 2013). An estimated 30-40% of aerosols at northern mid latitudes at 7-12 km altitudes originate from aircraft (Righi et al., 2013). In measurement campaigns concentrations of ultrafine (radii > 5 nm) was found to be 180-830 cm^{-3} for the southern hemisphere and 450-15000 cm^{-3} in the northern in the upper troposphere and aitken mode aerosols (radii > 14 nm) 130-400 cm^{-3} for the southern hemisphere and 290-9600 cm^{-3} in the northern respectively. Accumulation mode (0.5-2 μm) was lower at 6-34 cm^{-3} for the southern and 16-90 cm^{-3} in the northern hemispheres (Minikin et al., 2003). Other campaigns also showed a large variability in concentration in the subtropics, tropical tropopause and mid-latitudes between 50 and over 1000 cm^{-3} in 9-12 km altitudes (Borrmann et al., 2010). Other studies have focused on estimating the hygroscopicity of aerosols and cloud condensation nuclei. One study over the north China plain found average values in the range of 0.1-0.4 (Liu et al., 2014), the κ-parameter of water-soluble compounds has been found to be around 0.28 ± 0.06 according to (Padró et al., 2010).

https://doi.org/10.5194/egusphere-2025-3535
Preprint. Discussion started: 16 September 2025

3.1.4 The emulators for lubrication oil and aerosol activation

Capturing all this variation explicitly would lead to a very large number of particle types to include in the K15 model. Since the effect of ambient aerosols in hydrogen contrail formation has been studied to some extent previously (Bier et al., 2024) we have instead put our focus on the variability of lubrication oil. We thus handle the large variability of ambient aerosols, as done in previous studies (Kärcher et al., 2015; Bier et al., 2024), by lumping all together as one particle type with a representative size distribution and concentration. Ambient aerosols in addition to being activated also need time to get entrained into the plume. Our emulator of activated ambient aerosols at quench includes both entrainment and activation and gives the fraction of entrained activated ambient aerosols at quench given ambient conditions, represented by ambient temperature T_a, relative humidity rh, air pressure p_a and critical saturation temperature T_c (from SAC), more details can be found in supplementary S3.2.

The activation functions for lubrication oils and ambient aerosols, respectively, emulate the output at quench obtained by the K15 model when both lubrication oil and ambient aerosols are included. Examples of output from K15 and our emulators for different lognormal size distributions of lubrication oil and ambient aerosols at 60% relative humidity, for varying ambient temperatures are shown in Fig. 1. As seen in Fig. 1 the fit between the emulator and the output from the K15 is very good. The hardest cases for the emulators to capture are when the activation of lubrication oil is low which occurs for small mean radius and low hygroscopicity. Still, even in these cases the fit is decent, especially given the large uncertainties involved.

3.1.5 Base case implementation parameter values

The emulators are based on the K15 model and κ-Köhler theory and in our base case settings implemented with lubrication oil characteristics based on a lognormal size distribution with $\mu_o = 7.5$ nm and $\sigma_o = e^{0.375} \approx 1.45$ consistent with oil size distributions found in (Ungeheuer et al., 2022), where the oil was heated to 573K and then let to nucleate into droplets. This size-distribution for our base case is therefore on par with the oil being ejected into the main exhaust (we assume $T_0 = 660$K). In our base case the lubrication oil hygroscopicity is set to $\kappa_o = 6 \cdot 10^{-4}$, which is found as a maximum for lubrication oil in (Lambe et al., 2011). The base case lubrication oil droplet mass emission index we set to $\mathrm{EI}_o = 2$ mg (kg fuel)$^{-1}$ based on two studies. The first of these studies on kerosene engines shows an increase in oil emission index with power and an emission index range of 2-12 mg (kg fuel)$^{-1}$ (Yu et al., 2010). The other study found rather little dependence on power and emission indices in the range of 1-2 mg (kg fuel)$^{-1}$ with an outlier engine at 40 mg (kg fuel)$^{-1}$ (Timko et al., 2014) and highly dependent on the type of engine and the type of lubrication oil. Both studies have measured droplets of lubrication oil, thus only allowing the lubrication oil which has managed to form droplets to be measured. A third study estimated the oil emission index from the amount used by the engine and obtained a much higher estimate of 110 mg (kg fuel)$^{-1}$ (Decker et al., 2024).

For lognormal size distribution for the ambient aerosol we set the mean radius to $\mu_a = 15$ nm and standard deviation $\sigma_a = 2.2$ in line with (Kärcher et al., 2015) to cover a broad range of particle sizes. The hygroscopicity value is set to $\kappa_a = 0.5$ and the ambient concentration to $n_a = 1000$ cm^{-3} both values quite high ($n_a = 600$ cm^{-3} used in (Bier et al., 2024) for example) in order to not underestimate the impact of ambient aerosols' contribution to ice particle formation.

https://doi.org/10.5194/egusphere-2025-3535
Preprint. Discussion started: 16 September 2025

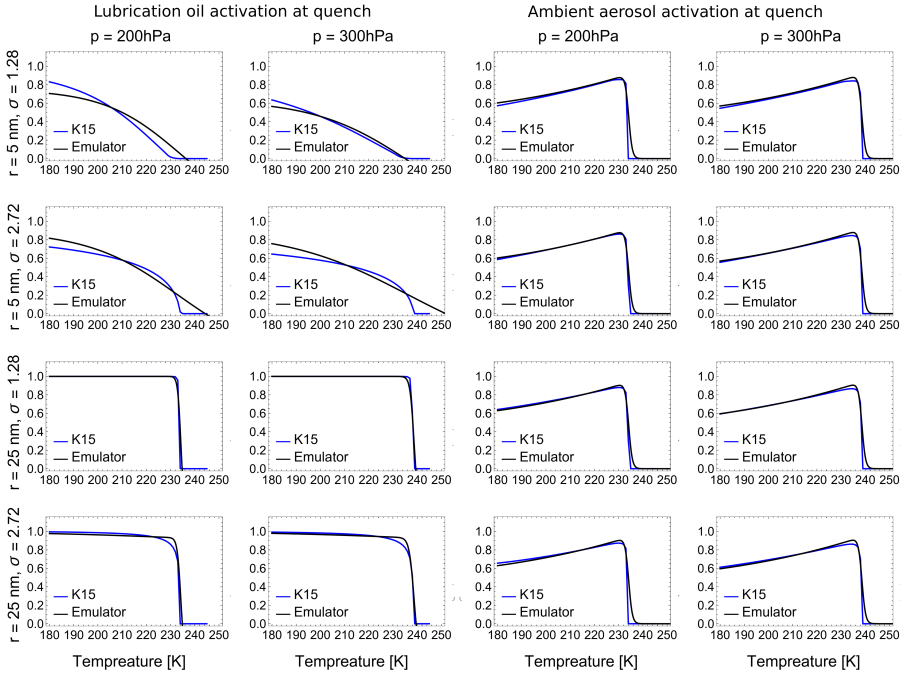

Figure 1. The figure shows examples from our emulators of lubrication oil activation to the left and ambient aerosol entrainment + activation to the right together with activation output from the K15 model for relative humidity at 60% and different lubrication oil size distributions (rows). The lower activation due to the Kelvin effect for small particles (mean radius r = 5 nm) is clearly seen for lubrication oil in the top two rows. The lower entrainment + activation values for ambient aerosols at low temperatures is due to lower entrainment because of shorter times before quench at low temperatures.

It should be noted that we are using the emulator of the K15 model under the conditions (small particle sizes and low hygroscopicity for lubrication oil) where the K15 model and hence our emulators, most certainly overestimates the amount of activated particles. Hence, the number of ice particles formed from lubrication oil will likely be slightly overestimated, especially for size distributions with small mean radius and for small values for the standard deviation.

In cases when we simulate contrail formation for fossil jet fuel we do not use K15 for the activation, but the standard approach in CoCiP. However, if the K15 model had been used to find the activation of soot and ambient aerosols for fossil jet fuel combustion we get activation almost identical to the activation function used in CoCiP for soot, see supplementary S6.

3.2 Contrail Cirrus Prediction model

CoCiP is a Lagrangian plume model that simulates contrail cirrus formation, development and climate impact in terms of energy forcing and radiative forcing (Schumann, 2012). It can be run either along flight paths or in a gridded mode with a test flight flying 1 km in the middle of the grid cells. For the simulation and calculations of contrail cirrus, CoCiP incorporates meteorological data and flight performance parameters. Any aircraft performance calculator can be used such as Eurocontrols

https://doi.org/10.5194/egusphere-2025-3535
Preprint. Discussion started: 16 September 2025

BADA family (Nuic et al., 2010) but CoCiP also has a built in aircraft performance model, the Poll-Schumann model (Poll and Schumann, 2021a, b, 2025) to obtain the performance variables such as fuel flow and engine efficiency, and non-volatile particulate matter (nvPM) emission number.

CoCiP utilises a monodisperse particle size distribution of ice particles once formed. The number of ice particles obtained from activation share the ice water content of the plume equally and properties of the plume, for example sedimentation rate, are calculated using an effective mean ice particle volumetric radius (Schumann, 2012). Radiative forcing however is calculated using different habits (shapes) of ice particles. CoCiP uses distributions of ice particle habits with up to three different habits out of eight possible, depending on the effective volumetric radius and based on when different habits are assumed to be prevalent. The habits have their own calculated effective radius and thus reflective area, such that the habit distribution influences the optical depth and the radiative forcing of the contrail cirrus (Schumann et al., 2011, 2012).

In this study we use the gridded version of CoCiP from the open-source pycontrails repository (v0.54.1). When running in gridded mode a model aircraft is chosen. We chose to use the aircraft with ICAO aircraft designator B737. It is one of the most common aircraft families (B73X) and also default in CoCiP grid. We use CoCiPs built in aircraft performance model the Poll-Schumann model. This means we obtain soot emission numbers for jet propulsion in the order of $\sim 10^{15}$ in the high soot regime. One could argue a comparison to lower soot emission numbers would be preferable mimicking a future kerosene fleet (in the same time-frame as a possible hydrogen fleet). In the lower soot regime however, there are still large uncertainties regarding the ability of ultrafine emission particles to form ice particles, significantly so at low temperatures, resulting in an increase in climate impact from contrail cirrus (Kärcher and Yu, 2009; Yu et al., 2024). Therefore we chose to make our comparison with the well known effects of jet aircraft in the high soot regime.

In this first implementation of hydrogen in CoCiP we use the built in CoCiP hydrogen fuel and our emulators for lubrication oil and ambient aerosol ice particle activation although we do not model a hydrogen aircraft, meaning we use the same B737 aircraft performance output such as true airspeed, aircraft weight for kerosene as well as for hydrogen fuel. This is a simplification for an actual hydrogen aircraft. Hydrogen has a higher energy content per unit mass than kerosene but a lower energy per unit volume and is in gas phase at atmospheric flight level conditions. Most hydrogen aircraft conceptual models and prototypes utilise compressed and cold liquid hydrogen which leads to fuel systems with higher complexity and tank volumes still larger than for kerosene. A measure of fuel system efficiency often used is Gravimetric Index (GI = fuel weight at full tank / (fuel weight at full tank + fuel system weight) reported in percent), measuring the share of fuel weight to the entire fuel system. Fuel system usually refers to all structures needed to store fuel such as tanks and piping. For jet fuel, the gravimetric index is close to 100% because the tanks are integrated into the wings. A bit simplified, lower gravimetric index adds to weight and drag of the aircraft increasing both power and energy needed for same flight patterns as jet flights.

To simulate the implications of different GI we utilise two modifications for hydrogen fuel on energy expenditure and fuel flow. Either we use energy expenditure corresponding to 1.6 times the energy expenditure for kerosene (Energy Consumption Ratio, ECR$= 1.6$) giving an upper estimation consistent with GI$= 20\%$ and energy usage in (Adler and Martins, 2023) (same GI gives approximately ECR$= 1.2$ for mid-range aircraft in (Mukhopadhaya and Rutherford, 2022)). This corresponds to a modification of fuel flow for hydrogen according to $\mathrm{ff}_{\mathrm{H}_2} \approx 0.56\ \mathrm{ff}_{\mathrm{J}}$ because of the higher energy content per mass. In a more

https://doi.org/10.5194/egusphere-2025-3535
Preprint. Discussion started: 16 September 2025

optimistic modification we set the energy consumption ratio to one (ECR$= 1$) consistent with a gravimetric index of GI$= 55\%$ and the break even point in (Adler and Martins, 2023) (and CoCiP default for hydrogen fuel). We anticipate that an actual hydrogen aircraft will fall somewhere in between these fuel flow boundaries and leave an accurate modelling of the energy use of a hydrogen fleet to future studies.

As meteorological input we use the high resolution (HRES) ERA5 reanalysis data provided by the European Center for Medium-range Weather Forecasts (ECMWF) (Hersbach et al., 2020) for the year 2019. The HRES ERA5 data has a latitude longitude resolution of $0.25° \times 0.25°$ and pressure levels between 1-1000 hPa. We have used either a range of flight levels of 100-600 hPa or the most common flight levels 200-300 hPa for different investigations. One of the important variables in the ERA5 dataset is relative humidity with respect to ice (RHi), which determines if a contrail will persist or not. Studies have highlighted that ERA5 RHi are usually weakly supersaturated and tend to underestimate high supersaturations compared to measurements (Gierens et al., 2020; Rädel and Shine, 2010; Reutter et al., 2020). When running CoCiP we therefore use the humidity scaling proposed by (Teoh et al., 2022a) included in the pycontrails package.

When we run CoCiP with hydrogen as fuel we utilise our emulators for lubrication oil activation A_o and ambient aerosol activation A_a. We obtain the ice particle number per meter N_{ice} for both lubrication oil and ambient aerosols according to

$$N_{\text{ice}} = \left(A_o \frac{ff}{v_{\text{tas}}} EI_{\text{n,o}} + A_a n_a A_{\text{plume}} n_{\text{engine}} \right) f_{\text{surv}}, \tag{5}$$

where ff (kg s^{-1}) is the fuel flow, v_{tas} (m s^{-1}) the true airspeed, $EI_{\text{n,o}}$ ((kg fuel)$^{-1}$) the lubrication oil droplet number emission index, n_a (m^{-3}) the ambient aerosol concentration, A_{plume} (m^2) the cross-sectional area of the plume at quench, n_{engine} the number of engines of the aircraft and f_{surv} CoCiPs survival fraction after the vortex downwash. More details can be found in supplementary S4. This is the ice particle number per meter after the downwash.

The more important parameter choices for our base case are listed in Table 1 more detailed parameter setting for the models can be found in supplementary Table S1.

4 Results

4.1 Comparing contrail cirrus climate effect from jet and hydrogen combustion aircraft.

To compare contrail cirrus climate effects generated by fossil jet fuel and hydrogen combustion aircraft we simulate contrail cirrus formation and properties for the whole year of 2019 on a global grid with 1 degree latitude and longitude resolution for both types of fuel. Our base parameter settings for hydrogen for ice particle formation are shown in Table 1. Equivalent parameters for fossil jet fuel, such as nvPM emission index, are generated in the aircraft performance module in CoCiP. In Fig. 2 we show in panel (a) and (b) the global 2019 probability of persistent contrail cirrus, (c) and (d) average contrail lifetime, and (e) and (f) average Energy Forcing per contrail generating flight meter (EFpcm), for both fuels (Hydrogen left column, fossil jet fuel right column) averaged over longitude, for latitude vs. altitude. As can be seen, the general patterns are similar between the two fuels, although there are some notable differences. As expected from the SAC the probability of contrail cirrus is higher at lower altitudes for hydrogen than for fossil jet fuel due to the larger emission intensity of water vapour for

https://doi.org/10.5194/egusphere-2025-3535
Preprint. Discussion started: 16 September 2025

Table 1. Parameter settings for our base case of hydrogen combustion.

Parameter	Notation	Value	Unit
Ambient aerosol mean radius	μ_a	15	nm
Ambient aerosol standard deviation	σ_a	2.20	nm
Ambient aerosol hygroscopicity parameter	κ_a	0.5	-
Ambient aerosol concentration	n_a	1000	cm^{-3}
Lubrication oil mean radius	μ_o	7.5	nm
Lubrication oil standard deviation	σ_o	$e^{0.375} \approx 1.45$	nm
Lubrication oil hygroscopicity parameter	κ_o	$6 \cdot 10^{-4}$	-
Lubrication oil droplet emission index	EI_o	2	mg (kg fuel)$^{-1}$
Engine exhaust temperature	T_0	660	K
Gravimetric index	GI	55	%
Energy consumption ratio ($E_{\mathrm{H}_2}/E_{\mathrm{J}}$)	ECR	1	-

hydrogen. Further, a shorter average contrail lifetime of hydrogen contrail cirrus is clearly seen when comparing panels (c) and (d) of Fig. 2. The shorter lifetime is because a smaller number of ice particles are activated for hydrogen combustion than for fossil jet combustion. This implies that more ice will deposit on each ice particle (in CoCiP the available ice water content is shared equally by all particles), which in turn implies that the mass of the particle will grow faster and also will sediment faster causing a reduction in contrail lifetimes (Lewellen et al., 2014; Kärcher, 2016). The lower lifetimes in turn contributes to the lower EFpcm seen for hydrogen compared to jet in the (e) and (f) panels respectively (note the difference in scale).

Although lower average contrail lifetime does contribute to a lower EFpcm the largest decrease comes from the reduction in the reflective area of all ice particles following the lower number of ice particles for hydrogen combustion compared to fossil jet fuel combustion. The ice particles still share the same ice water content (as discussed above) but the area to volume ratio drops with a smaller number of particles. The reduced ice particle area reduces the optical depth and thereby radiative forcing and energy forcing (Lewellen et al., 2014; Kärcher, 2016).

In Fig. 3 we see the average ice particle numbers for hydrogen and jet after downwash for altitude vs. latitude. For hydrogen the ice particle contributions from lubrication oil and ambient aerosols are shown separately in panels (b) and (a) respectively in Fig. 3. Ice particle number from lubrication oil is seen to be lowest at lower altitudes because of higher temperatures leading to lower supersaturations in the plume in general and lower activation of the lubrication oil droplets. On the contrary ice particle numbers from ambient aerosols show an increase at lower altitudes. This is because the limiting factor for ambient aerosols is rather the time window for particles to get entrained into the plume. With lower activation of lubrication oil it takes longer to quench the supersaturation of the plume and hence more ambient aerosols can be entrained and activated and form ice particles at higher temperatures/lower altitudes. This activation behaviour can be seen in Fig. 1 where the activation for ambient aerosols

https://doi.org/10.5194/egusphere-2025-3535
Preprint. Discussion started: 16 September 2025

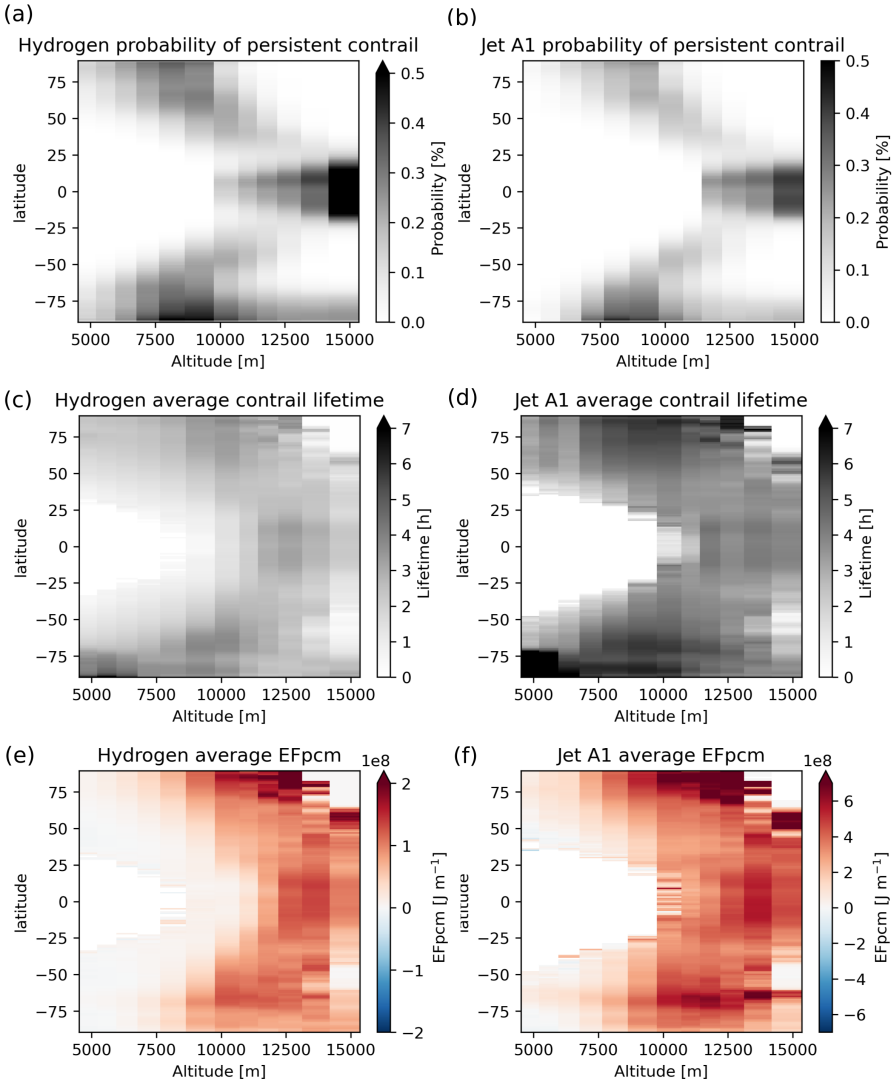

Figure 2. Comparison of 2019 longitudinal averages between jet and hydrogen persistent contrail cirrus. Top panels (a) and (b) show the probability of persistent contrails. The middle panels (c) and (d) show the average contrail lifetime and the bottom panels (e) and (f) show average energy forcing per contrail forming flight meter (EFpcm). Note the difference in scale for the EFpcm between hydrogen and jet plots. Hydrogen simulations are run with with base setting $GI = 55$, $\kappa = 6 \cdot 10^{-6}$, $\mathrm{EI}_o = 2$ mg (kg fuel)$^{-1}$ and lognormal size distribution LogNormal($\mu_o = 7.5$ nm, $\sigma_o \approx 1.45$) for lubrication oil and, $\kappa = 0.5$ and LogNormal($\mu_a = 15$ nm,$\sigma_a = 2.2$) for ambient aerosols.

is seen to drop at lower temperatures. The ice particle number for jet is more than 5 times larger than for hydrogen over the whole span of latitudes and altitudes where fossil jet fuel SAC is fulfilled.

To better see the total potential impacts of hydrogen and fossil jet fuel aircraft we combine the effect of contrail cirrus formation probability and EFpcm, and estimate the average Energy Forcing per flight meter (EFpfm). The result is shown in

https://doi.org/10.5194/egusphere-2025-3535
Preprint. Discussion started: 16 September 2025

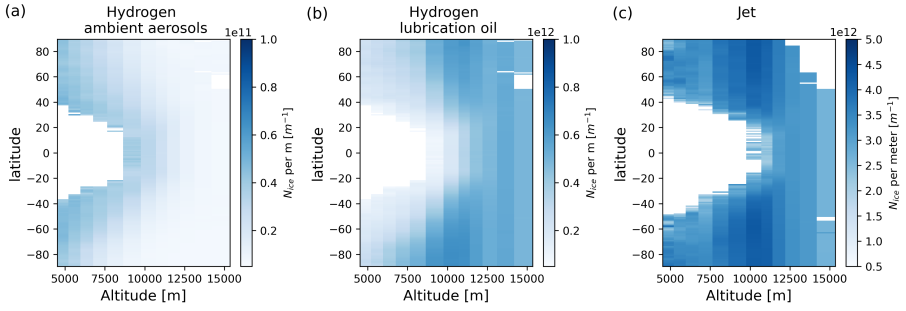

Figure 3. Comparison of average number of ice particles per meter between jet and hydrogen contrail cirrus (with ambient aerosol (a) and lubrication oil (b) ice particles separated for hydrogen) after the vortex downwash. Note the difference in scale between all three plots. Hydrogen simulations are run with base setting GI$= 55$, $\kappa = 6 \cdot 10^{-6}$, $\mathrm{EI}_o = 2$ mg (kg fuel)$^{-1}$ and size distribution LogNormal($\mu_o = 7.5$ nm, $\sigma_o \approx 1.45$) for lubrication oil and, $\kappa = 0.5$ and LogNormal($\mu_a = 15$ nm, $\sigma_a = 2.2$) for ambient aerosols. All simulations are run for 20 randomly chosen dates (see supplementary S5) as a representative sample for year 2019.

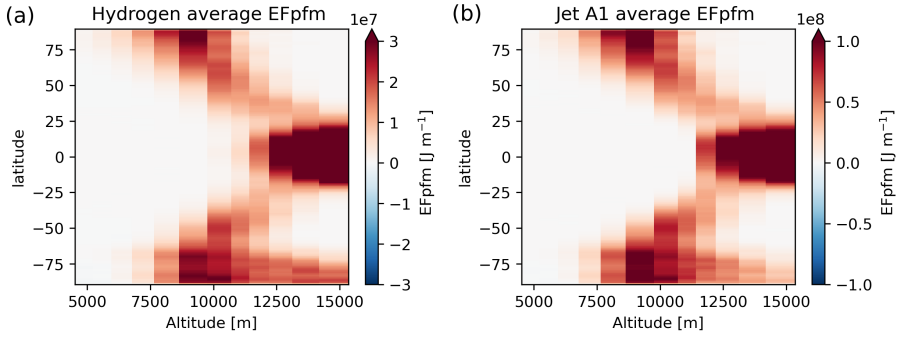

Figure 4. Comparison of average EFpfm between jet (b) and hydrogen (c) persistent contrails. Note the difference in scale between the plots. Hydrogen simulations are run with with base setting GI$= 55$, $\kappa = 6 \cdot 10^{-6}$, $\mathrm{EI}_o = 2$ mg (kg fuel)$^{-1}$ and size distribution, LogNormal($\mu_o =$ 7.5nm, $\sigma_o \approx 1.45$), for lubrication oil and, $\kappa = 0.5$ and LogNormal($\mu_a = 15$ nm,$\sigma_a = 2.2$) for ambient aerosols.

Fig. 4 for both hydrogen (a) and jet (b) aircraft and we see that even if the probability of formation is larger for hydrogen, this only has a noticeable impact on relatively low altitudes. However, it is a modest effect, hard to discern in Fig. 4. The patterns again look similar for the two fuels, but the colour intensity used in the figure is different and the scale for fossil jet fuel is higher than that of hydrogen.

https://doi.org/10.5194/egusphere-2025-3535
Preprint. Discussion started: 16 September 2025

4.2 Impact of lubrication oil size distributions

4.2.1 Lubrication oil sensitivity analysis

To get an improved understanding of how the average contrail EF for hydrogen combustion aircraft depend on the parametrization of lubrication oil size distributions and other key uncertainties we perform a sensitivity analysis. In these simulations, we use the same 20 randomly chosen dates (see supplementary S5) as a representative sample for year 2019 for all simulations. The ambient aerosol concentration is kept constant at the base setting for all simulations. For the lubrication oil we use a span of mean radius μ_o from 5 nm to 25 nm in steps of 5 nm and the standard deviation σ_o between $e^{0.25} \approx 1.28$ and $e^{1.0} \approx 2.72$ in steps of $e^{0.25}$. For these spans of mean and standard deviation we investigate our base settings with lubrication oil hygroscopicity parameter $\kappa_o = 6 \cdot 10^{-4}$, oil droplet mass emission index $\mathrm{EI}_o = 2$ mg (kg fuel)$^{-1}$ and energy consumption ratio ECR$= 1$. In addition we test three additional cases 1) with hygroscopicity parameter changed to $\kappa_o = 0.1$, 2) oil droplet mass emission index $\mathrm{EI}_o = 20$ mg (kg fuel)$^{-1}$ and 3) the Energy consumption ratio ECR$= 1.6$. A hygroscopicity parameter as high as 0.1 is quite unreasonable for lubrication oil but it is assumed so as to better understand the sensitivity to our base assumption. One case of oil droplet emission mass index of $\mathrm{EI}_o = 40$ mg (kg fuel)$^{-1}$ was measured in (Yu et al., 2010), although all other values lay in the range 0.1-3 mg (kg fuel)$^{-1}$. A value of $\mathrm{EI}_o = 20$ mg (kg fuel)$^{-1}$ is therefore not out of range but quite extreme.

Average energy forcings per flight meter covering latitudes 70°S-70°N, all longitudes and flight levels 300-200 hPa (ca 9000-12000 m) for the 20 dates during 2019 are calculated and shown in the first row of Fig. 5. A first observation is that there are a few cases for which hydrogen contrail cirrus have higher EFpfm than conventional fossil jet fuel of today. This occurs when assuming a high lubrication oil emission intensity or a high κ combined with size distribution assumptions with small standard deviation and small mean radius. For high oil emission intensity this is due to the large number of oil droplets available. Even if the Kelvin effect leads to a smaller share of oil droplets activated into ice particles, which can be seen from the smaller increase in ice particles per meter between 10 nm and 5 nm (e), a large number can still be formed. The high κ has a large impact for small mean radius and variance since it enables a larger share of the droplets available to activate.

In general we can see in Fig 5 that distributions with small mean radius and variance have larger average EFpfm (see first column and small mean radius). The high EFpfm is seen to drop off quite rapidly as mean radius (follow the x-axis to the right in each panel) and standard deviation are increased (as shown by the different columns). The high EFpfm for small radius and variance is again due to the larger number of oil droplets that can activate into water droplets, which can be seen in the second row as ice particles per meter after downwash. Since the ice water content of the plume for all cases, except the case with higher ECR, is the same and that in CoCiP, this water content is assumed to be shared equally among the particles formed, more particles lead to smaller particles as noted in Sec. 4.1 and seen in the last row of Fig. 5 where we show ice particle radius averaged over contrail cirrus lifetime. Smaller average particles sediment more slowly and thereby give longer contrail cirrus average lifetimes in general as can be seen in row three of Fig. 5. There are exceptions to this, since evaporation also plays a role in contrail cirrus lifetime. We can see this for the high lubrication oil emission case where the contrail cirrus lifetime is seen to be lower for $\mu_o = 5$ nm in comparison to $\mu_o = 10$ nm for small σ_o ((i) and (j)). Here the ice particles are small enough that evaporation shortens the contrail cirrus average lifespan.

https://doi.org/10.5194/egusphere-2025-3535
Preprint. Discussion started: 16 September 2025

In row four of Fig. 5 we show the optical depth averaged over contrail cirrus lifetime for all cases. We see that, in general the high ice particle number cases also lead to high optical depth. A noticeable break in this trend is the lower optical depth for fossil jet fuel compared to high oil emission and high κ for $\sigma \approx 1.28$ despite a larger number of ice particles per meter after downwash.

It is also interesting that the assumptions of technical proficiency (GI, fuel flow and ECR) have a rather modest effect in comparison to the oil droplet mass emission index. The increase in EFpfm is smaller than 1.6 for the lower gravimetric index. This is due to the larger ice water content for the higher ECR leading to proportionally larger ice particle losses in the wake vortex downwash of CoCiP.

4.2.2 Ambient Aerosol contribution to ice particle formation

The contribution of ambient aerosols to the formation of ice particles in absolute numbers varies slightly depending on the size distribution and amount of oil droplets. For a large amount of oil droplets present, the droplets quickly deplete the available water and "quench" the plume leaving little time for ambient aerosols to be entrained into the plume and contribute to ice particle formation. For such cases both the relative share of ice particles formed on ambient aerosols and absolute number are smaller although the absolute number marginally so. In fact ice particles from ambient aerosols is almost the same magnitude for all cases as seen in Fig. 6, where we show the average numbers of ice particles from lubrication oil (b) and ambient aerosols (a) after downwash as well as ambient aerosol ice particle number percentage (c) for all cases and size distributions. In cases where there are fewer oil droplets present at formation the ambient aerosols contribute with a larger share and in the case with oil size distributions with large means and variances the ambient aerosols are responsible for the majority of ice particles.

The end point of our ranges with $\mu_o = 25$ nm and $\sigma_o \approx 2.72$, which gives the lowest number of oil particles, can be seen as a rough estimate of the average EFpfm for ambient aerosols alone (an exception is the case when we assume a high oil emission index).

5 Discussion

Our analysis of contrail cirrus impacts of hydrogen as aviation fuel indicates the possibility of a significant climate benefit. For almost all parameter settings considered we find that hydrogen offers a reduction in energy forcing per flight meter compared to conventional jet aircraft, with a global average reduction of about 70% using our base case assumptions. For our base case we find an average ice particle reduction of approximately 85% compared to conventional jet while a reduction of more than 80-90% was found in (Bier et al., 2024) for hydrogen combustion with only ambient aerosols as ice nuclei. One may further note that SAF is expected to reduce the number of ice particles. One study found a 49% reduction for 100% SAF (Teoh et al., 2022b). However, the ice particle number in our study, is highly dependent on the lubrication oil size distribution and lubrication oil emission index. We find a few percent of reduction in the worst case of high oil emission index and high hygroscopicity, small lubrication oil mean radius and a small standard deviation for ice particle number after downwash, but

https://doi.org/10.5194/egusphere-2025-3535
Preprint. Discussion started: 16 September 2025

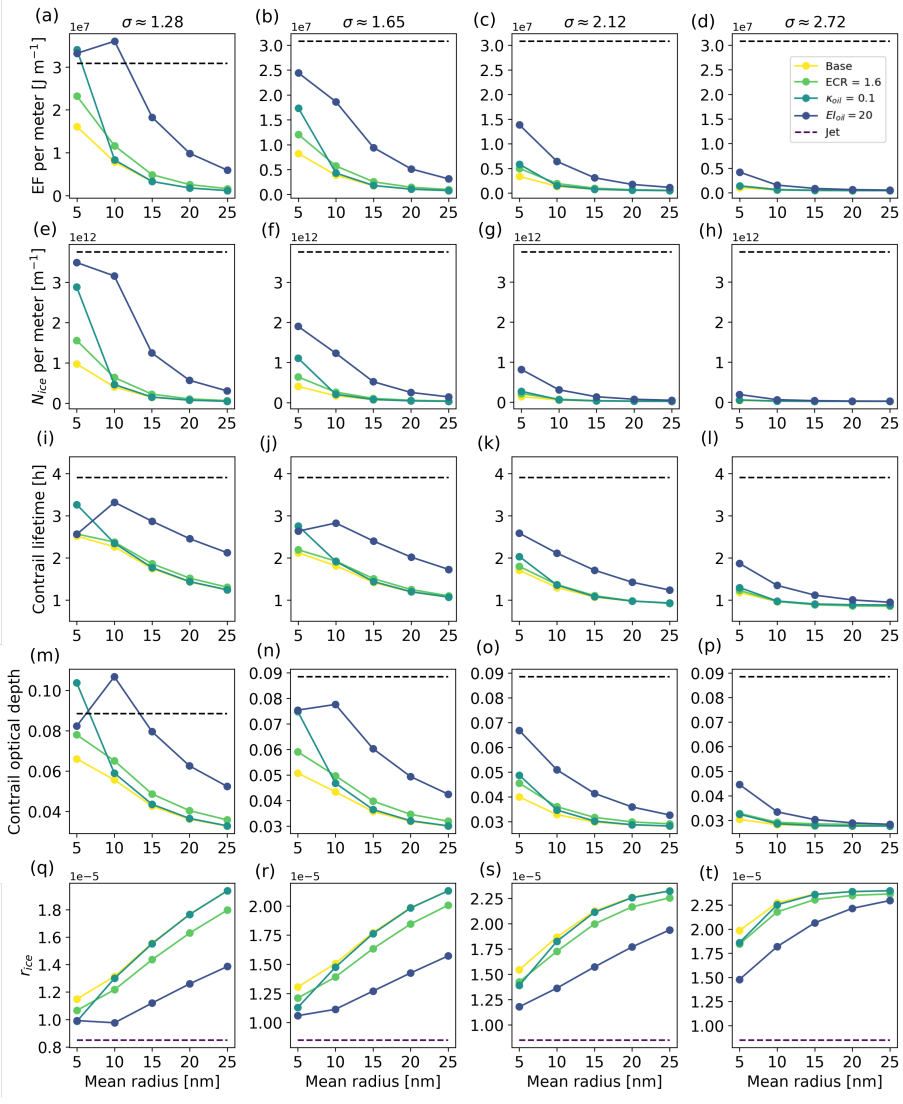

Figure 5. The figure shows average energy forcing per flight meter (row 1), average number of ice particles per meter after downwash (row 2), average contrail lifetime (row 3), contrail optical depth averaged over contrail cirrus lifetime (row 4) and ice particle radius averaged over contrail cirrus lifetime (row 5) for different lognormal size distribution radii (x-axis) and standard deviation (the columns) for four cases of lubrication oil parameters; base setting (yellow), larger fuel flow for hydrogen (light green), large lubrication oil hygroscopicity (dark green) and high oil emission index (dark blue). For comparison black striped lines show the average for fossil jet fuel. All simulations are run for the same set of 20 randomly chosen dates.

up to around 99% reduction for larger oil droplets when lubrication oil is vented rather than emitted in the main exhaust. This shows the possibilities and importance of future hydrogen engines design for a low contrail cirrus climate impact.

https://doi.org/10.5194/egusphere-2025-3535
Preprint. Discussion started: 16 September 2025

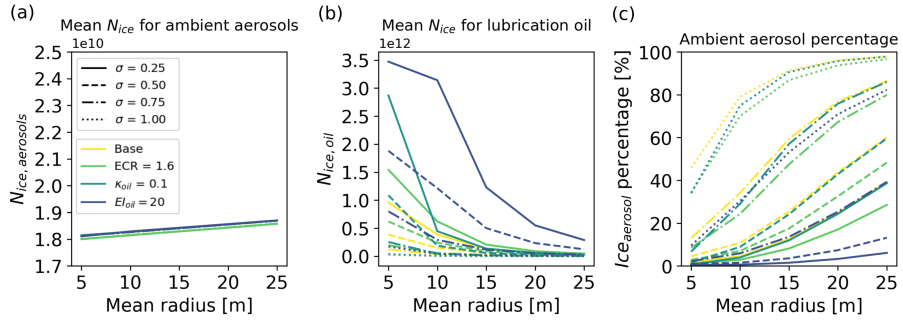

Figure 6. The figure shows the average number of ice particles after downwash stemming from ambient aerosols to the left (a) and lubrication oil in the middle (b) as well as ambient aerosol ice number percentage to the right (c) for all cases as a function of the lubrication oil size distributions.

Despite the reduction in the majority of cases there are uncertainties and caveats in the modelling approach used. CoCiP is a simplified model and although it has been calibrated and compared (with relatively good fit) against data (Schumann et al., 2017), these data are mainly from the middle part of the contrail cirrus life-time and the comparison might therefore not capture the full effect of the contrail cirrus. A recent comparison between CoCiP and APCEMM (Akhtar Martínez et al., 2025) highlights that a substantial part of the contrail cirrus later life-time might be missed in the CoCiP model. This leads to a lower estimate of the life-time optical depth (proxy for climate impact) in CoCiP compared to APCEMM by approximately a factor 4.

For APCEMM a large part of the life-time optical depth in the model comes from the latest stages of contrail cirrus life-time which is hard to measure with various instruments due to low optical depth. It is still uncertain if APCEMM or CoCiP is closer to the real world. However, APCEMM fall-streak behaviour is largely in agreement with more resolved models than CoCiP (Unterstrasser and Gierens, 2010; Lewellen et al., 2014; Lewellen, 2014).

If contrail cirrus lifespan is modelled to be too short in CoCiP the most affected contrail cirrus would be those with high initial ice water content and low ice particle numbers which, in the model, generate large ice particles with a fast sedimentation. Since CoCiP does not employ size distributions, all particles sediment at the same rate, with the consequence that a longer lived tail of smaller particles are missed. Since high ice water content and fewer particles at formation is possible for hydrogen combustion, there is a risk of a relatively larger underestimation of energy forcing per meter for hydrogen (for cases with broader distributions with larger mean radii in our study) than for fossil jet fuel in CoCiP.

From the theoretical K15 model in (Kärcher et al., 2015) for ice particle formation we expect an overestimation of ice particles due to the "quench"-procedure where all water droplets form at once rather than a successive activation of particles into water droplets. A successive activation would successively deplete the supersaturation, thus lowering it under the activation threshold for small particles and particles with low hygroscopicity.

The magnitude of overestimation due to the K15 model and the underestimation because of possibly shorter lifespan due to the modelling approach in CoCiP is difficult to estimate. There are no observations of ice particle formation from hydrogen

https://doi.org/10.5194/egusphere-2025-3535
Preprint. Discussion started: 16 September 2025

flight yet against which to compare our ice particle estimates. Although, the first measurement campaign of contrail formation from hydrogen aircraft was launched in December 2024 and with its upcoming publication we can better understand the modelling caveats. As mentioned above the latest stages of contrail cirrus life-time is largely unmeasured due to low optical depth.

An interesting finding in our study is the relatively small difference in EF per flight meter between our base case and the more technically pessimistic assumption of a lower gravimetric index with an increase in energy usage by a factor of 1.6. It is also worth noting that if our base case hygroscopicity underestimates the actual hygroscopicity of lubrication oil or if there are versions with higher κ, this would not increase the climate impact to any significant degree. The prominent factor, is the amount of particles present for ice particle formation, as shown in Fig. 5 in terms of emission index and lubrication oil size distribution. Although there is a saturation effect, as seen with the higher lubrication oil emission index for small radii and narrow distributions, that could be alleviated with more favourable circumstances for activation with higher ECR or higher hygroscopicity. In general though, an increase in ice water content as with low gravimetric index, high hygroscopicity and to some extent smaller particles have a smaller effect than the number of particles that can act as condensation nuclei.

As the main determining factor for the magnitude of energy forcing per meter is the amount of particles present for ice particle formation rather than the properties of the particles, it indicates that our simplified approach to handle ambient aerosols is good enough for the purpose of the study. We assumed that the ambient aerosols could be described by single lognormal distribution using a single hygroscopicity. We intentionally did set the ambient aerosol concentration high and assumed a relatively high hygroscopicity value so that the ice particle contribution from ambient aerosols are at the high end.

However, there are locations where the concentration is even higher measuring up to 15000 cm^{-3} in the upper troposphere of the northern hemisphere for ultrafine particles with radii < 5 nm (Minikin et al., 2003). This, however, is in general a local occurrence and high ice particle numbers would be hindered to some degree by the Kelvin effect in activation.

Despite the uncertainties our study indicates the possibility of substantial climate benefits in terms of reduced contrail cirrus EF per flight meter for hydrogen in comparison to conventional jet. In addition, our parameter sweep over lubrication oil size distributions give guidance for future hydrogen engine design. Releasing lubrication oil in the main exhaust at high temperatures should be avoided and there is a potentially large climate benefit in more efficient recapturing schemes and venting (if necessary) as far away from the exhaust as possible to minimize entrainment into the plume.

6 Conclusions

Our results indicate that contrail cirrus from hydrogen combustion aircraft generate significantly lower energy forcing than those from fossil jet fuel combustion under a majority of settings. The primary mechanism is a reduced number of particles available to act as ice nuclei. While fossil jet fuel combustion emits soot and other volatile particulate matter that dominate ice nucleation, contrail formation from hydrogen combustion depends instead on lubrication oil particles and ambient aerosols serving as condensation nuclei.

https://doi.org/10.5194/egusphere-2025-3535
Preprint. Discussion started: 16 September 2025

We show that ice particle formation on lubrication oil and ambient aerosols can be captured using activation emulators based on the microphysical framework proposed by Kärcher et al. (Kärcher et al., 2015). Although lubrication oil may partially compensate for the absence of soot, its effectiveness as an ice nucleus is highly sensitive to poorly constrained factors such as its emission index and particle size distribution. Nonetheless, the conclusion that hydrogen combustion leads to lower contrail cirrus energy forcing remains robust across a wide range of assumptions regarding lubrication oil properties.

Overall, our findings suggest that hydrogen aircraft may offer not only CO_2-free propulsion but also substantially reduced non-CO_2 climate impacts from contrail cirrus, provided that lubrication oil emissions are effectively controlled. Engine design should therefore treat lubrication oil handling as a critical parameter.

Code and data availability. Contrail model codes and generated data are available for scientific research purposes from the authors upon request and partly found at https://doi.org/10.5281/zenodo.15874256.

Author contributions. SP and DJ designed the study. SP carried out the simulations, analysis and the preparation of the manuscript. DJ helped with the analysis. DJ and CA contributed to the preparation of the manuscript.

Competing interests. The authors declare no conflict of interests.

Acknowledgements. Funding has been provided by VINNOVA grant number 2023-01286, Chalmers Area of Advance Transport.

https://doi.org/10.5194/egusphere-2025-3535
Preprint. Discussion started: 16 September 2025

References

Adler, E. J. and Martins, J. R.: Hydrogen-powered aircraft: Fundamental concepts, key technologies, and environmental impacts, Progress in Aerospace Sciences, 141, 100 922, 2023.

Akhtar Martínez, C., Eastham, S. D., and Jarrett, J. P.: Contrail models lacking post-fallstreak behavior could underpredict lifetime optical depth, EGUsphere, 2025, 1–26, 2025.

Bier, A., Unterstrasser, S., Zink, J., Hillenbrand, D., Jurkat-Witschas, T., and Lottermoser, A.: Contrail formation on ambient aerosol particles for aircraft with hydrogen combustion: a box model trajectory study, Atmospheric Chemistry and Physics, 24, 2319–2344, 2024.

Borrmann, S., Kunkel, D., Weigel, R., Minikin, A., Deshler, T., Wilson, J. C., Curtius, J., Volk, C. M., Homan, C. D., and Ulanovsky, A.: Aerosols in the tropical and subtropical UT/LS: in-situ measurements of submicron particle abundance and volatility, Atmospheric Chemistry and Physics, 10, 5573–5592, 2010.

Clarke, A. D. and Kapustin, V. N.: A Pacific aerosol survey. Part I: A decade of data on particle production, transport, evolution, and mixing in the troposphere, Journal of the atmospheric sciences, 59, 363–382, 2002.

Decker, Z. C., Alpert, P. A., Ammann, M., Anet, J. G., Bauer, M., Cui, T., Durdina, L., Edebeli, J., Gysel-Beer, M., and Pre´vo ̂t, A. S.: Emission and Formation of Aircraft Engine Oil Ultrafine Particles, ACS EST Air, 1, 1662–1672, 2024.

Durdina, L., Brem, B. T., Elser, M., Scho¨nenberger, D., Siegerist, F., and Anet, J. G.: Reduction of nonvolatile particulate matter emissions of a commercial turbofan engine at the ground level from the use of a sustainable aviation fuel blend, Environmental Science Technology, 55, 14 576–14 585, 2021.

Fushimi, A., Saitoh, K., Fujitani, Y., and Takegawa, N.: Identification of jet lubrication oil as a major component of aircraft exhaust nanoparticles, Atmospheric Chemistry and Physics, 19, 6389–6399, 2019.

Gierens, K., Matthes, S., and Rohs, S.: How well can persistent contrails be predicted?, Aerospace, 7, 169, 2020.

Hersbach, H., Bell, B., Berrisford, P., Hirahara, S., Horányi, A., Muñoz-Sabater, J., Nicolas, J., Peubey, C., Radu, R., and Schepers, D.: The ERA5 global reanalysis, Quarterly journal of the royal meteorological society, 146, 1999–2049, 2020.

Kaiser, J. C., Hendricks, J., Righi, M., Jöckel, P., Tost, H., Kandler, K., Weinzierl, B., Sauer, D., Heimerl, K., and Schwarz, J. P.: Global aerosol modeling with MADE3 (v3. 0) in EMAC (based on v2. 53): model description and evaluation, Geoscientific Model Development, 12, 541–579, 2019.

Kärcher, B.: The importance of contrail ice formation for mitigating the climate impact of aviation, Journal of Geophysical Research: Atmospheres, 121, 3497–3505, 2016.

Kärcher, B. and Yu, F.: Role of aircraft soot emissions in contrail formation, Geophysical Research Letters, 36, 2009.

Kärcher, B., Turco, R., Yu, F., Danilin, M., Weisenstein, D., Miake-Lye, R., and Busen, R.: A unified model for ultrafine aircraft particle emissions, Journal of Geophysical Research: Atmospheres, 105, 29 379–29 386, 2000.

Kärcher, B., Burkhardt, U., Bier, A., Bock, L., and Ford, I.: The microphysical pathway to contrail formation, Journal of Geophysical Research: Atmospheres, 120, 7893–7927, 2015.

Kölker, K., Zengerling, Z., Kühlen, M., Lütjens, K., and Linke, F.: Assessing the impact of contrail avoidance through rescheduling on airline network flows: A case study of North Atlantic flights, Transportation Research Part A: Policy and Practice, 187, 104 155, 2024.

Lambe, A., Onasch, T., Massoli, P., Croasdale, D., Wright, J., Ahern, A., Williams, L., Worsnop, D., Brune, W., and Davidovits, P.: Laboratory studies of the chemical composition and cloud condensation nuclei (CCN) activity of secondary organic aerosol (SOA) and oxidized primary organic aerosol (OPOA), Atmospheric Chemistry and Physics, 11, 8913–8928, 2011.

https://doi.org/10.5194/egusphere-2025-3535
Preprint. Discussion started: 16 September 2025

Lee, D. S., Fahey, D. W., Skowron, A., Allen, M. R., Burkhardt, U., Chen, Q., Doherty, S. J., Freeman, S., Forster, P. M., and Fuglestvedt, J.: The contribution of global aviation to anthropogenic climate forcing for 2000 to 2018, Atmospheric Environment, 244, 117 834, 2021.

Lewellen, D.: Persistent contrails and contrail cirrus. Part II: Full lifetime behavior, Journal of the Atmospheric Sciences, 71, 4420–4438, 2014.

Lewellen, D., Meza, O., and Huebsch, W.: Persistent contrails and contrail cirrus. Part I: Large-eddy simulations from inception to demise, Journal of the Atmospheric Sciences, 71, 4399–4419, 2014.

Lewellen, D. C.: A large-eddy simulation study of contrail ice number formation, Journal of the Atmospheric Sciences, 77, 2585–2604, 2020.

Liu, H., Zhao, C., Nekat, B., Ma, N., Wiedensohler, A., Van Pinxteren, D., Spindler, G., Müller, K., and Herrmann, H.: Aerosol hygroscopicity derived from size-segregated chemical composition and its parameterization in the North China Plain, Atmospheric Chemistry and Physics, 14, 2525–2539, 2014.

Minikin, A., Petzold, A., Ström, J., Krejci, R., Seifert, M., van Velthoven, P., Schlager, H., and Schumann, U.: Aircraft observations of the upper tropospheric fine particle aerosol in the Northern and Southern Hemispheres at midlatitudes, Geophysical Research Letters, 30, 2003.

Moore, R. H., Thornhill, K. L., Weinzierl, B., Sauer, D., D'Ascoli, E., Kim, J., Lichtenstern, M., Scheibe, M., Beaton, B., and Beyersdorf, A. J.: Biofuel blending reduces particle emissions from aircraft engines at cruise conditions, Nature, 543, 411–415, 2017.

Mukhopadhaya, J. and Rutherford, D.: Performance analysis of evolutionary hydrogen-powered aircraft, ICCT white paper, 2022.

Nuic, A., Poles, D., and Mouillet, V.: BADA: An advanced aircraft performance model for present and future ATM systems, International journal of adaptive control and signal processing, 24, 850–866, 2010.

Padró, L. T., Tkacik, D., Lathem, T., Hennigan, C. J., Sullivan, A. P., Weber, R. J., Huey, L. G., and Nenes, A.: Investigation of cloud condensation nuclei properties and droplet growth kinetics of the water-soluble aerosol fraction in Mexico City, Journal of Geophysical Research: Atmospheres, 115, 2010.

Petters, M. and Kreidenweis, S.: A single parameter representation of hygroscopic growth and cloud condensation nucleus activity, Atmospheric Chemistry and Physics, 7, 1961–1971, 2007.

Poll, D. and Schumann, U.: An estimation method for the fuel burn and other performance characteristics of civil transport aircraft in the cruise. Part 1 fundamental quantities and governing relations for a general atmosphere, The Aeronautical Journal, 125, 257–295, 2021a.

Poll, D. and Schumann, U.: An estimation method for the fuel burn and other performance characteristics of civil transport aircraft during cruise: part 2, determining the aircraft's characteristic parameters, The Aeronautical Journal, 125, 296–340, 2021b.

Poll, D. and Schumann, U.: An estimation method for the fuel burn and other performance characteristics of civil transport aircraft; part 3 full flight profile when the trajectory is specified, The Aeronautical Journal, pp. 1–37, 2025.

Ponsonby, J., King, L., Murray, B. J., and Stettler, M. E.: Jet aircraft lubrication oil droplets as contrail ice-forming particles, Atmospheric Chemistry and Physics, 24, 2045–2058, 2024.

Quante, G., Voigt, C., and Kaltschmitt, M.: Targeted use of paraffinic kerosene: Potentials and implications, Atmospheric Environment: X, p. 100279, 2024.

Raes, F., Van Dingenen, R., Vignati, E., Wilson, J., Putaud, J.-P., Seinfeld, J. H., and Adams, P.: Formation and cycling of aerosols in the global troposphere, Atmospheric environment, 34, 4215–4240, 2000.

Reutter, P., Neis, P., Rohs, S., and Sauvage, B.: Ice supersaturated regions: properties and validation of ERA-Interim reanalysis with IAGOS in situ water vapour measurements, Atmospheric chemistry and physics, 20, 787–804, 2020.

https://doi.org/10.5194/egusphere-2025-3535
Preprint. Discussion started: 16 September 2025

Righi, M., Hendricks, J., and Sausen, R.: The global impact of the transport sectors on atmospheric aerosol: simulations for year 2000 emissions, Atmospheric Chemistry and Physics, 13, 9939–9970, 2013.

Rosenow, J. and Fricke, H.: Luchkova et al. Minimizing contrail formation by rerouting around dynamic ice-supersaturated regions, Aeron Aero Open Access J, 2, 105–111, 2018.

Rädel, G. and Shine, K. P.: Validating ECMWF forecasts for the occurrence of ice supersaturation using visual observations of persistent contrails and radiosonde measurements over England, Quarterly Journal of the Royal Meteorological Society, 136, 1723–1732, 2010.

Schumann, U.: On conditions for contrail formation from aircraft exhausts, Meteorologische Zeitschrift, 5, 4–23, 1996.

Schumann, U.: A contrail cirrus prediction model, Geoscientific Model Development, 5, 543–580, 2012.

Schumann, U., Mayer, B., Gierens, K., Unterstrasser, S., Jessberger, P., Petzold, A., Voigt, C., and Gayet, J.-F.: Effective radius of ice particles in cirrus and contrails, Journal of the Atmospheric Sciences, 68, 300–321, 2011.

Schumann, U., Mayer, B., Graf, K., and Mannstein, H.: A parametric radiative forcing model for contrail cirrus, Journal of Applied Meteorology and Climatology, 51, 1391–1406, 2012.

Schumann, U., Baumann, R., Baumgardner, D., Bedka, S. T., Duda, D. P., Freudenthaler, V., Gayet, J.-F., Heymsfield, A. J., Minnis, P., and Quante, M.: Properties of individual contrails: a compilation of observations and some comparisons, Atmospheric Chemistry and Physics, 17, 403–438, 2017.

Stier, P., Feichter, J., Kinne, S., Kloster, S., Vignati, E., Wilson, J., Ganzeveld, L., Tegen, I., Werner, M., and Balkanski, Y.: The aerosol-climate model ECHAM5-HAM, Atmospheric Chemistry and Physics, 5, 1125–1156, 2005.

Teoh, R., Schumann, U., Gryspeerdt, E., Shapiro, M., Molloy, J., Koudis, G., Voigt, C., and Stettler, M.: Aviation contrail climate effects in the North Atlantic from 2016–2021, 2022a.

Teoh, R., Schumann, U., Voigt, C., Schripp, T., Shapiro, M., Engberg, Z., Molloy, J., Koudis, G., and Stettler, M. E.: Targeted use of sustainable aviation fuel to maximize climate benefits, Environmental Science Technology, 56, 17 246–17 255, 2022b.

Timko, M. T., Albo, S. E., Onasch, T. B., Fortner, E. C., Yu, Z., Miake-Lye, R. C., Canagaratna, M. R., Ng, N. L., and Worsnop, D. R.: Composition and sources of the organic particle emissions from aircraft engines, Aerosol Science and Technology, 48, 61–73, 2014.

Ungeheuer, F., Caudillo, L., Ditas, F., Simon, M., van Pinxteren, D., Kılıç, D., Rose, D., Jacobi, S., Kürten, A., and Curtius, J.: Nucleation of jet engine oil vapours is a large source of aviation-related ultrafine particles, Communications Earth Environment, 3, 319, 2022.

Unterstrasser, S. and Gierens, K.: Numerical simulations of contrail-to-cirrus transition–Part 1: An extensive parametric study, Atmospheric Chemistry and Physics, 10, 2017–2036, 2010.

Voigt, C., Kleine, J., Sauer, D., Moore, R. H., Bräuer, T., Le Clercq, P., Kaufmann, S., Scheibe, M., Jurkat-Witschas, T., and Aigner, M.: Cleaner burning aviation fuels can reduce contrail cloudiness, Communications Earth Environment, 2, 114, 2021.

Yang, P., Hong, G., Dessler, A. E., Ou, S. S., Liou, K.-N., Minnis, P., and Harshvardhan: Contrails and induced cirrus: Optics and radiation, Bulletin of the American Meteorological Society, 91, 473–478, 2010.

Yu, F. and Turco, R. P.: The role of ions in the formation and evolution of particles in aircraft plumes, Geophysical Research Letters, 24, 1927–1930, 1997.

Yu, F., Turco, R. P., and Kärcher, B.: The possible role of organics in the formation and evolution of ultrafine aircraft particles, Journal of Geophysical Research: Atmospheres, 104, 4079–4087, 1999.

Yu, F., Karcher, B., and Anderson, B. E.: Revisiting contrail ice formation: Impact of primary soot particle sizes and contribution of volatile particles, Environmental Science Technology, 2024.

https://doi.org/10.5194/egusphere-2025-3535
Preprint. Discussion started: 16 September 2025

Yu, Z., Liscinsky, D. S., Winstead, E. L., True, B. S., Timko, M. T., Bhargava, A., Herndon, S. C., Miake-Lye, R. C., and Anderson, B. E.: Characterization of lubrication oil emissions from aircraft engines, Environmental science technology, 44, 9530–9534, 2010.

Zhang, C., Chen, L., Ding, S., Zhou, X., Chen, R., Zhang, X., Yu, Z., and Wang, J.: Mitigation effects of alternative aviation fuels on non-volatile particulate matter emissions from aircraft gas turbine engines: A review, Science of The Total Environment, 820, 153 233, 2022.